

# Dispersion blue-shift in an aperiodic Bragg reflection waveguide

Volodymyr I. Fesenko<sup>a,\*</sup>, Vladimir R. Tuz<sup>a</sup>

<sup>a</sup>*Institute of Radio Astronomy of National Academy of Sciences of Ukraine, Kharkiv, Ukraine*

---

## Abstract

A particular feature of an aperiodic design of cladding of Bragg reflection waveguides to demonstrate a dispersion blue-shift is elucidated. It is made on the basis of a comparative study of dispersion characteristics of both periodic and aperiodic configurations of Bragg mirrors in the waveguide system, wherein for the aperiodic configuration three procedures for layers alternating, namely Fibonacci, Thue–Morse and Kolakoski substitutional rules are considered. It was found out that, in a Bragg reflection waveguide with any considered aperiodic cladding, dispersion curves of guided modes appear to be shifted to shorter wavelengths compared to the periodic configuration regardless of the modes polarization.

*Keywords:* photonic crystals, Bragg reflection waveguide, aperiodic structure, dispersion characteristics

*PACS:* 42.25.Bs, 42.70.Qs, 42.79.Gn, 42.82.Et

---

## 1. Introduction

As is known, in contrast with conventional optical waveguides based on the effect of the total internal reflection inside a high-index core [1], distinctive features of Bragg reflection waveguides are influenced by a multilayered configuration of their composite cladding [2], which has a form of a stack of alternating high- and low-index layers. Indeed, such a composition of cladding

---

<sup>\*</sup>Institute of Radio Astronomy of National Academy of Sciences of Ukraine, 4, Chervonopraporna St., Kharkiv 61002, Ukraine

*Email address:* v.i.fesenko@ieee.org (Volodymyr I. Fesenko)

leads to formation of photonic bandgaps in the spectra of the multilayered system resulting in light confinement within a low-index core which is usually considered to be an air gap. Such photonic bandgap guidance brings several attractive features to the waveguide characteristics [3, 4], in particular, since most of light is guided inside a low-index core, losses and nonlinear effects can be significantly suppressed compared to the conventional high-index guiding waveguides.

Furthermore, even in the simplest symmetric configuration of Bragg reflection waveguides there is a set of unique optical features that are unattainable in conventional waveguides since the former ones are highly dispersive due to their complicate geometry (rather than just to their material composition). As such features we can mention that in Bragg reflection waveguides [5, 6]: (i) each guided mode has several cutoff points, which results in ability to design a waveguide supported only the high-order modes instead of the fundamental one; (ii) there is a possibility to lose a specific mode due to shrinking of the photonic bandgap into point; (iii) some specific modes with negative order can appear when a system consists of a thin enough guiding layer. On the other hand, Bragg reflection waveguides exhibit an extra degree of freedom for optimizing their optical characteristics through utilization of particular designs of the cladding, among which an asymmetric mirrors design [7, 8], layers chirping in the cladding [9, 10], and placing the matched layers between the core and cladding [11] may be referred.

In this paper we report on the other possibility of tuning the operation bandwidth of Bragg reflection waveguides by applying an another special design to the multilayered cladding. Our motivation in this study is in follows. If we have a look from the viewpoint of practical applications, both the number of layers in the cladding and their thicknesses should be as small as possible. It is due to the fact that the production of waveguides with thinner layers requires fewer amount of materials for deposition, and thus less time for the process. At the same time, it contradicts with the technological limits that are imposed on the possibility of producing layers with a very small thicknesses. Besides, it is difficult to reach precise step-index profiles with sharp boundaries, and this problem is more significant for structures with the thinnest layers. In this context, it is of interest to find such a configuration of layers in the cladding, which would allow one to shift the operation frequency of the waveguide into the higher band without changing number of layers and their thicknesses.

It is obvious that through the solution of an optimization problem [12] it

is possible to find the best spatial distribution of layers in a random sequence that produces a maximal shift, however, in this consideration we prefer to deal with deterministically ordered structures instead of completely random ones, since in the first case we are able to definitely predict the spectral properties of the system [13, 14, 15, 16, 17], i.e. the width and position of stopbands on the frequency scale, which are key characteristics that are taken into consideration when designing the Bragg reflection waveguides. As noted in our previous papers [18, 19, 20, 21], stopbands in the spectra of aperiodic structures can appear to be shifted in comparison with the stopbands in the spectra of periodic structures assuming the same material parameters and number of layers in the multilayered systems. Therefore, in this paper, in order to provide a comparative study, we consider spectral features and dispersion characteristics of a Bragg reflection waveguide having either periodic or aperiodic configuration of layers in the cladding. For an aperiodic configuration we have a choice between three well known aperiodic chains produced through substitution rules of Fibonacci [22], Thue–Morse [23], and Kolakoski [24] sequences.

## 2. Theoretical Description

We consider a Bragg reflection waveguide (Fig. 1a) that is made of a low-index core layer (in particular, an air gap) sandwiched between two identical either periodic or aperiodic one-dimensional Bragg mirrors formed by stacking together layers of two different sorts  $\Psi$  and  $\Upsilon$ , which have thicknesses  $d_\Psi$ ,  $d_\Upsilon$  and refractive indices  $n_\Psi$  and  $n_\Upsilon$ , respectively. The numbers of constitutive layers of each sort are defined as  $N_\Psi$  and  $N_\Upsilon$ . The structure inhomogeneity (i.e. the variation of the refractive index) extends along the  $z$ -axis, and in this direction the system is finite, i.e. we suppose that mirrors on either side of the core layer consist of a finite number  $N$  of the constitutive layers. In other two directions  $x$  and  $y$  the structure is invariant and infinite. In such a geometry the axis of symmetry of the structure under study corresponds to the middle of the core layer which is at the line  $z = 0$ , where the core layer has thickness  $2d_g$  and refractive index  $n_g$ .

Therefore, we study a Bragg reflection waveguide having a core layer with thickness  $2d_g = \lambda_{qw}/2n_g$ , where  $\lambda_{qw} = 1\mu\text{m}$ . As constituents for the cladding composition we utilize a combination of layers made of GaAs and oxidized AlAs, whose refractive indices at the given wavelength  $\lambda_{qw}$  are  $n_\Psi = 3.50$  and  $n_\Upsilon = 1.56$ , respectively. The thicknesses  $d_\Psi$  and  $d_\Upsilon$  are chosen to be 74.5 nm

for GaAs layers and 208.2 nm for AlAs-oxide layers in order to provide the operation bandwidth to be within the first telecommunication window.

As an aperiodic configuration three alternative designs of the waveguide's mirrors are investigated. Thus, a comparative study between the waveguides with the multilayered cladding altered according to the substitutional rules of Fibonacci [22], Thue–Morse [23], and Kolakoski [24] sequences is provided (see, Appendix A).

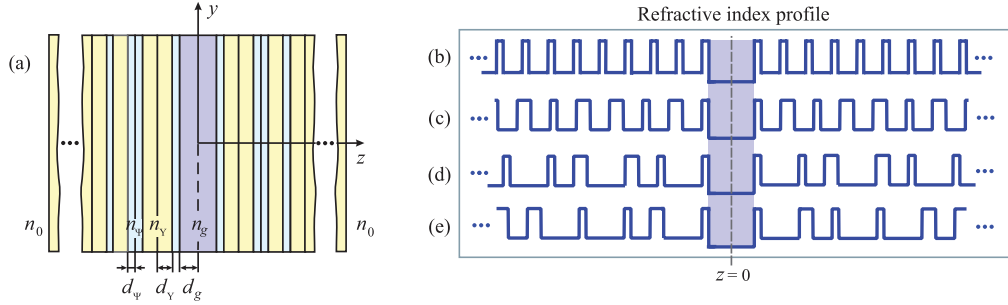


Figure 1: (a) The schematic of a symmetrical Bragg reflection waveguide that consists of a core layer sandwiched between two aperiodic mirrors. Index profiles of the waveguide's cladding where layers are arranged according to the generation rules of (b) periodic, (c) Fibonacci, (d) Thue–Morse, and (e) Kolakoski sequences.

In the chosen structure configuration, each guided mode of TE polarization  $\{E_x, H_y, H_z\}$  or TM polarization  $\{H_x, E_y, E_z\}$  propagates along the  $y$ -axis with its own propagation constant  $\beta$ . As the mirrors on each side of the waveguide core layer are the same (i.e. the Bragg reflection waveguide is symmetrical about the  $z$ -axis,  $n(-z) = n(z)$ ), as it is depicted in Fig. 1 b-e), the equations for waves travelling back and forth inside the channel regardless of the type of polarization can be joined on the boundaries  $z = d_g$  and  $z = -d_g$  into the next system

$$\begin{cases} a_0 \exp(-ik_{zg}d_g) = Rb_0 \exp(ik_{zg}d_g), \\ b_0 \exp(-ik_{zg}d_g) = Ra_0 \exp(ik_{zg}d_g), \end{cases} \quad (1)$$

from which the relation between amplitudes can be found

$$b_0 = a_0 R \exp(2ik_{zg}d_g). \quad (2)$$

Here  $k_{zg} = k_0(n_g^2 - n_{eff}^2)^{1/2}$  is the transverse wavenumber in the core,  $n_{eff} = \beta/k_0$  is introduced as an effective refractive index for each particular guided

mode,  $k_0 = \omega/c$  is the free space wavenumber, and  $R$  is the complex reflection coefficient of the Bragg mirror which is depended on the wave polarization. The reflection coefficient  $R$  can be derived engaging the transfer matrix formalism [18, 19, 20] (see, Appendix B).

Eliminating amplitudes  $a_0$  and  $b_0$  from system (1), the dispersion equation for the guided modes of the Bragg reflection waveguide is obtained as

$$1 - R^2 \exp \left[ 4ik_0 d_g \sqrt{n_g^2 - n_{eff}^2} \right] = 0. \quad (3)$$

This equation is further solved numerically to find out a function of the propagation constant  $\beta$  versus frequency  $\omega$ . The resulting propagation constant  $\beta$  is sought in the field of complex numbers due to the existence of intrinsic losses in the waveguide constitutive materials and energy leakage through the outermost layers because the number of layers  $N$  in the Bragg mirrors is a finite quantity.

The proper selection of the constitutive materials suggests the preference of substances with low internal losses. According to [26] the imaginary parts of the dielectric constants of the chosen GaAs and oxidized AlAs are negligibly small within the wavelength region of interest. Therefore, the main source of losses in the Bragg reflection waveguides under consideration is the energy leakage through their finite cladding. These losses can be estimated via the expression [5]:

$$\text{Loss[dB/cm]} = \frac{-\lambda \ln |R|}{40n_g d_g^2 \sqrt{1 - (\lambda/4n_g d_g)^2}}. \quad (4)$$

From our estimation for the lowest modes presented in Fig. 2 it follows that the level of losses decreases exponentially with  $N$  (see, also discussions on this matter in [5, 27]), and leakage of the TM mode is much greater than that of the TE mode. The leakage is also greater for the waveguides with an aperiodic arrangement of the cladding compared with the periodic system. Thus, the criterion of smallness of the imaginary part of  $\beta$  when classifying the waveguide modes can be satisfied by setting the number  $N$  to an appropriate high value.

For the symmetric waveguides all guided modes can be divided into symmetric and anti-symmetric ones. Without loss of generality, the overall field amplitude in the middle line of the core can be reduced to unity or zero for symmetric and anti-symmetric modes, respectively. Then the field in the

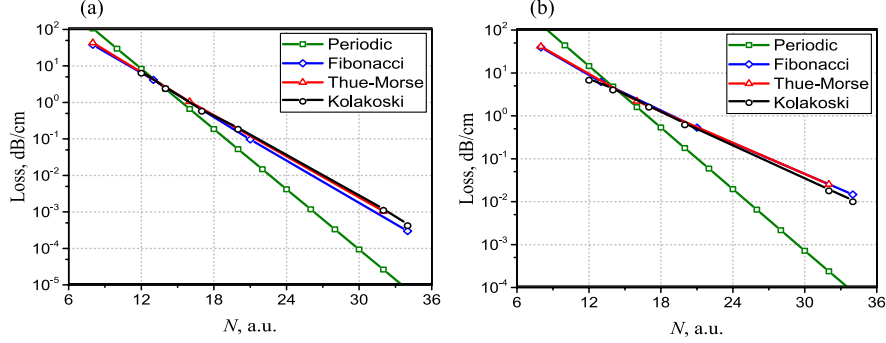


Figure 2: Estimation of the energy leakage in the Bragg reflection waveguides with either periodic or aperiodic configuration of layers in the finite cladding; (a) TE mode and (b) TM mode;  $n_g = 1$ .

core can be normalized by setting  $a_0 = 1/2$  and  $b_0 = \pm 1/2$ , where the upper sign ‘+’ is related to symmetric modes, while the lower sign ‘−’ is related to anti-symmetric ones, respectively.

### 3. Numerical Results: Solution Analysis

Our goal here is to demonstrate a dispersion blue-shift of guided modes in a Bragg reflection waveguide that appears in the system having aperiodically arranged layers in the cladding. In order to reveal the mentioned blue-shift we provide a comparative study of the waveguide with either periodic or aperiodic configuration of the cladding. It is supposed that the periodic Bragg mirrors consist of a finite number of layers ( $N = 32$ ) which is enough to provide the desired level of reflection in order to guarantee that the propagation constant  $\beta$  is essentially real. Obviously, the number of layers of each sort  $\Psi$  and  $\Upsilon$  in the periodic system is the same ( $N_\Psi = N_\Upsilon = 16$ ). Further three aperiodic designs are investigated. In the first aperiodic configuration the mirrors are formed by stacking together layers  $\Psi$  and  $\Upsilon$  according to the Fibonacci generation rule on its eighth generation stage. At this stage there are  $N = 34$  layers in the system with different number of layers of each sort  $\Psi$  and  $\Upsilon$  ( $N_\Psi = 21$  and  $N_\Upsilon = 13$ ). In the second configuration, the cladding is arranged according to the Thue–Morse substitution rule on its six generation stage which corresponds to the system with the same number of layers as in the periodic configuration ( $N = 32$ ). There is the same number of layers

of each sort  $\Psi$  and  $\Upsilon$  in this system ( $N_\Psi = N_\Upsilon = 16$ ). As the third configuration, the cladding is considered to be an aperiodic structure arranged according to the Kolakoski  $K(1, 2)$  generation scheme on its twentieth generation stage. For such a configuration the total number of layers coincides with those ones of the periodic and Thue–Morse structures ( $N = 32$ ), but there is different number of layers of each sort  $\Psi$  and  $\Upsilon$  ( $N_\Psi = 17$  and  $N_\Upsilon = 15$ ).

For clarity, we should note that the total number of layers and the number of layers of each sort within the deterministically aperiodic multilayered system depend on the generation stage, and for certain schemes it is impossible to obtain a given number of layers in the system (e.g., using the Fibonacci substitution rule it is impossible to obtain the system consisting of  $N = 32$  layers). Thereby, a complete coincidence in the layers numbers on the earlier generation stages exists only for periodic and Thue–Morse configurations, for these structures the different spatial order of the layers is the only difference between them. On the other hand, in the infinite limit of the generation stage the numbers of layers of each sort  $N_\Psi$  and  $N_\Upsilon$  in the periodic, Thue–Morse and Kolakoski structures take on the same values, while for the Fibonacci structure the numbers of layers can be calculated from the formulas [19] obtained using the generating functions technique [?]:  $N_\Psi = [(\tau^+)^{\sigma-2} - (\tau^-)^{\sigma-2}] / \sqrt{5}$ ,  $N_\Upsilon = [(\tau^+)^{\sigma-1} - (\tau^-)^{\sigma-1}] / \sqrt{5}$ , where  $\sigma$  is the generation stage ( $\sigma > 2$ ), and  $\tau^\pm = (1 \pm \sqrt{5})/2$ . Here  $\tau^+$  is the well known golden mean value [13].

In Fig. 3 both band diagrams and dispersion curves for TE and TM polarizations are presented. They are calculated for the waveguide whose core layer is an air gap surrounded by the cladding with either periodic (a, b) or aperiodic (c-h) arrangement. Here, regions colored in light green correspond to the bands within which light can propagate through the multilayered structure (passbands), whereas uncolored areas correspond to the bands where the level of reflection is high enough ( $|R| > 0.99$ ), therefore they can be identified as stopbands.

In this figure the guided modes are indicated by a set of colored (blue and black) points, and it is evident that all these guided modes appear only within the bands where the level of reflection reaches high values ( $|R| \geq 0.99$ ) (i.e. within the stopbands). One can conclude from Fig. 3, that the dispersion curve of each guided mode is terminated at the stopbands edge at either maximal or minimal allowable value of  $n_{eff}$ , at which there is a mode cutoff. Besides, it can be observed that for all aperiodic waveguide configurations the dispersion curves appear to be shifted to shorter wavelength (i.e. they

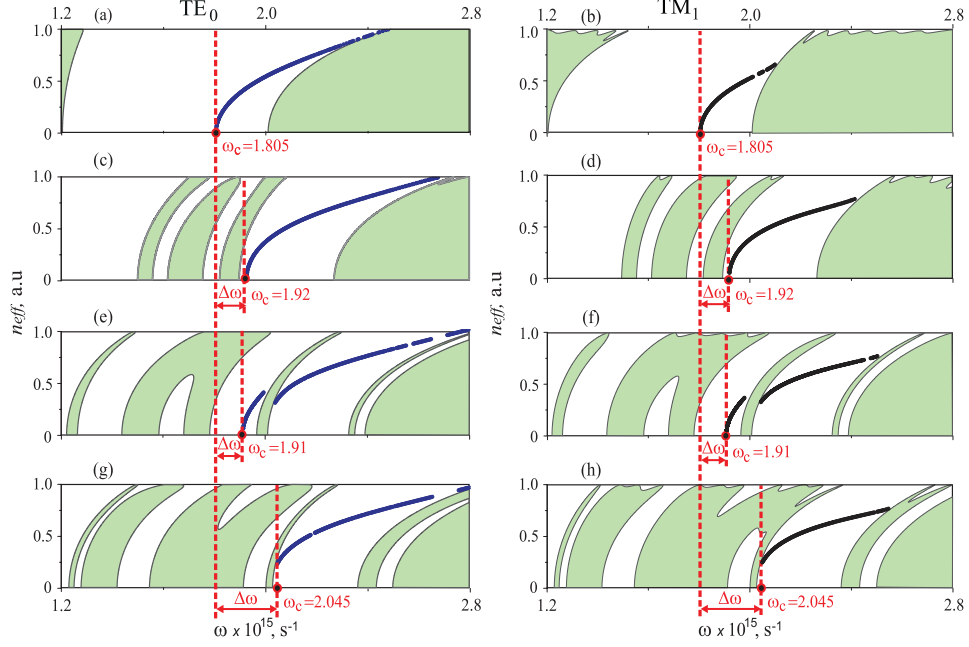


Figure 3: The band diagrams and dispersion curves for TE (left column) and TM (right column) polarizations in the Bragg reflection waveguide with either periodic or aperiodic configuration of layers in the cladding that are arranged according to different generation rules: (a, b) periodic; (c, d) Fibonacci; (e, f) Thue–Morse; (g, h) Kolakoski  $K(1, 2)$ . Blue and black dispersion curves correspond to  $TE_0$  and  $TM_1$  modes, respectively;  $\omega_c$  is a cutoff frequency;  $n_g = 1$ .

acquire some blue-shift which is marked in figures as  $\Delta\omega$ ) as compared to the dispersion curves related to the structure with the periodic arrangement. In fact this blue shift depends very little on the refractive index of the core layer as it is depicted in Fig. 4 (assuming of course that  $n_g$  is smaller than the refractive index  $n_T$  of the first layer in the mirrors).

We should note that generally stopbands which carry the above-mentioned modes are also shifted to shorter wavelength. It is a consequence of the fact that in contrast to periodic multilayered systems which have the main stopband centered around  $\lambda_{qw}$ , aperiodic structures are characterized by a set of (pseudo) stopbands which are distributed symmetrically around this wavelength accompanied with highly localized transmission peaks in the vicinity of the wavelength  $\lambda_{qw}$ .

Evidently, the dispersion shift appears due to different spatial orders of



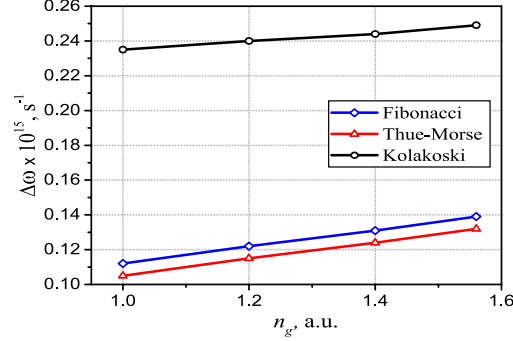


Figure 4: The blue shift of the cutoff frequency  $\omega_c$  versus the refractive index of the core layer.

the constitutive layers in the considered waveguide's configurations. Thus, the difference in order of arrangement of layers results in the optical thickness changing of particular layers in the structure, since some repetitions in a row of layers of the same sort  $\Psi$  or  $\Upsilon$  can appear in the aperiodic sequences that reduces the number of layers' interfaces within the system compared to the periodic one. The formation of layers with doubled thicknesses  $2d_\Psi$  and  $2d_\Upsilon$  produces the enlarged phase shift  $\phi_i$ , that leads to a change in the total reflection spectrum of the mirror, because the shape of the reflection spectrum of a multilayered structure depends on the phase modulation of each layer as  $\phi_i = 2\pi n_i d_i / \lambda_{qw}$ . If we mark the phase modulation for the doubled layers as  $\phi$ , then the reflectivity can be factorized as the product of two contributions  $R = A(n_\Upsilon/n_\Psi) \cdot \Re(\phi)$  [29], where the function  $A$  takes into account the value of the reflectivity due to the refractive index contrast, and  $\Re$  is a shape factor that represents the different optical paths of the light inside the layers. In our case, indeed, changes in  $\Re(\phi)$  result in the dispersion shift, since the substitution  $\Re(\phi(n_i, 2d_i)) \rightarrow \Re(\phi(n_i, d_i))$  takes place.

It is noticed in Fig. 3 that the longest shift is observed for the Bragg reflection waveguide whose cladding is formed according to the Kolakoski  $K(1, 2)$  generation rule due to the greater number of the doubled layers in the mirrors compared to other considered systems. For the given waveguide parameters, in wavelengths, the maximal shift is observed to be about 122 nm.

In order to prove that the obtained dispersion curves are associated to the same waveguide modes, the field profiles inside the waveguide for the

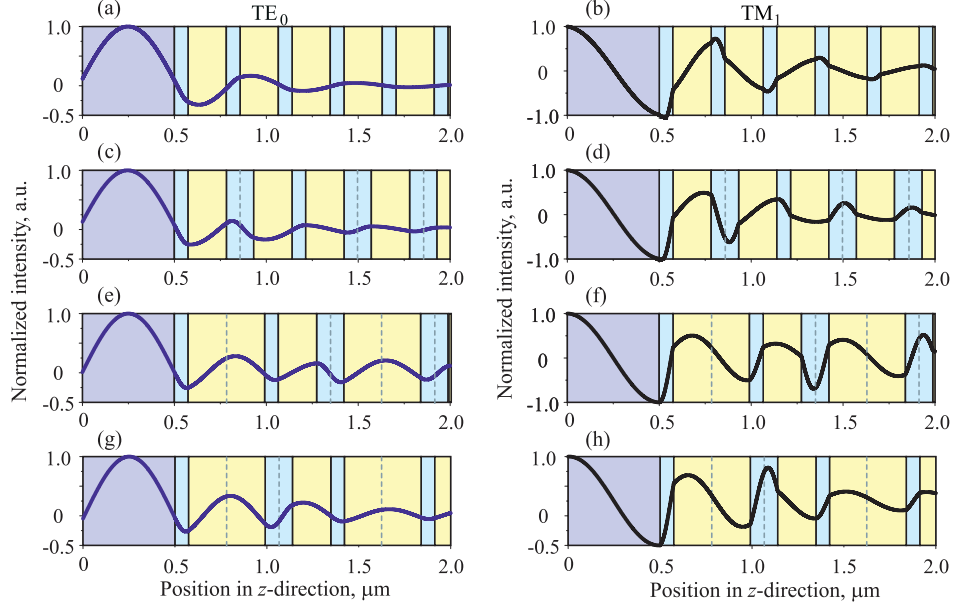


Figure 5: Intensity profile of the guided modes for different configurations of the cladding: (a, b) periodic; (c, d) Fibonacci; (e, f) Thue–Morse; (g, h) Kolakoski  $K(1, 2)$ . Blue curves correspond to the electric-field patterns related to the  $E_x$  component of the field for  $TE_0$  mode. Black curves correspond to the magnetic-field patterns related to the  $H_x$  component of the field for  $TM_1$  mode;  $n_g = 1$ . The confinement factor is: (a)  $\Gamma = 0.87$ ; (b)  $\Gamma = 0.61$ ; (c)  $\Gamma = 0.67$ ; (d)  $\Gamma = 0.44$ ; (e)  $\Gamma = 0.76$ ; (f)  $\Gamma = 0.57$ ; (g)  $\Gamma = 0.85$ ; (h)  $\Gamma = 0.59$ .

corresponding field components ( $E_x$  for TE mode, and  $H_x$  for TM mode) are calculated at the same frequency ( $\omega = 2.1 \times 10^{15} \text{ s}^{-1}$ ) which are reported in Fig. 5. These mode-field profiles are plotted after applying normalization of the field magnitude on its maximal value within the core. From these figures it follows, that the field of the fundamental  $TE_0$  mode appears to be well confined within the central air-guiding core. The degree of this confinement can be estimated via calculation of the confinement factor  $\Gamma = (\int_{-d_g}^{d_g} |I|^2 dz) / (\int_{-\infty}^{\infty} |I|^2 dz)$ , where  $I$  is related to field components  $E_x$  and  $H_x$  for TE modes and TM modes, respectively. Thus, the confinement factor related to the  $TE_0$  mode manifests rather high values for all discussed configurations (see, values of  $\Gamma$  given in the caption of Fig. 3) and, especially, the highest values 0.87 and 0.85 are obtained for the periodic and aperiodic Kolakoski  $K(1, 2)$  configurations of the cladding. Besides, the field intensity of the fundamental mode decays rapidly within the first few pairs of the con-

stitutive layers of the cladding as it is depicted in Fig. 3. At the same time, the field of  $\text{TM}_1$  mode appears to be less confined within the core layer, thus, as was already mentioned, the field leakage is higher for this polarization.

#### 4. Conclusions

To conclude, a dispersion blue-shift in a Bragg reflection waveguide consisting of an aperiodic design of layers in the cladding compared to the periodic design is demonstrated. The strength of this blue-shift is investigated for three aperiodic multilayered systems, namely for those alternated according to Fibonacci, Thue–Morse and Kolakoski substitution rules. It is recognized that the longest shift is observed for the Bragg reflection waveguide whose cladding is formed according to the Kolakoski  $K(1, 2)$  sequence.

In order to prove that the considered dispersion curves are associated to the same waveguide modes, both the field profile inside the waveguide and the confinement factor for each mode are calculated. It is found out that the highest confinement factor can be achieved in the Kolakoski  $K(1, 2)$  structure among other aperiodic designs.

We argue that the design of cladding in the form of an aperiodic structure gives rise to change in the dispersion characteristics, resulting in the shift of cutoff wavelengths of guided modes toward the shorter wavelength regardless of their polarization.

#### Appendix A. Aperiodic Orders

In optics, a standard algorithm for arranging aperiodic photonic structures is usually based on a certain symbolic substitution rule (i.e. on a specific substitution rule  $w$  that operates on a finite alphabet  $A$  which consists of a set of letters  $\{a, b, c, \dots\}$ ). In practical realizations each letter can be associated with a particular constitutive block (e.g. with a dielectric or semiconductor layer) in a resulting photonic structure. In this regard, substitution sequences that act upon a two-letter alphabet are especially important. Such algorithms can be reduced to following:

$$a \rightarrow w_1(a, b), \quad b \rightarrow w_2(a, b), \quad (\text{A.1})$$

where  $w_1$  and  $w_2$  can be any string of letters  $a$  and  $b$ .

Fibonacci sequence is obtained via iteration of the rule  $w_F$  [22], as

$$a \rightarrow ab, \quad b \rightarrow a, \quad (\text{A.2})$$

resulting in the letters chain  $\{a \rightarrow ab \rightarrow aba \rightarrow abaab \rightarrow abaababa \rightarrow \dots\}$ .

Thue–Morse sequence is generated by the substitution  $w_{TM}$  [23], as

$$a \rightarrow ab, \quad b \rightarrow ba, \quad (\text{A.3})$$

resulting in the letters chain  $\{a \rightarrow ab \rightarrow abba \rightarrow abbabaab \rightarrow \dots\}$ .

The generation rule  $w_K$  of the Kolakoski sequence is similar to those ones of Fibonacci and Thue–Morse sequences and can be based on two symbols substitution. Namely, the sequence  $K(a, b)$  can be obtained by starting with  $a$  as a seed and iterating the following two substitutions [24]

$$w_0 : \begin{array}{l} b \rightarrow a^b \\ a \rightarrow a^a \end{array} \quad \text{and} \quad w_1 : \begin{array}{l} b \rightarrow b^b \\ a \rightarrow b^a \end{array} \quad (\text{A.4})$$

where  $w_0$  and  $w_1$  can be any string of letters  $a$  and  $b$ ;  $a^b$  denotes a run of  $a$   $b$ 's, i.e.,  $a^b = a\dots a$  ( $b$  times). In this paper we examine the case when  $a = 1$  and  $b = 2$ , so the letters chain  $\{abbaababba\dots\}$  appears. Remarkably, using the Kolakoski substitutional rule (A.4) it is possible to obtain any value of the total number of letters in the resulting chain by changing its generation stage and starting letter of the sequence.

## Appendix B. Transfer Matrix Description

The plane monochromatic waves of TE ( $\vec{E}^{\text{TE}} \parallel \vec{x}_0$ ) and TM ( $\vec{H}^{\text{TM}} \parallel \vec{x}_0$ ) polarizations can be defined in a particular  $j$ -th layer ( $j = 1, 2, \dots, N$ ) of the sequence in the form

$$\begin{Bmatrix} \vec{E}_j^{\text{TE}} \\ \vec{H}_j^{\text{TM}} \end{Bmatrix} = \vec{x}_0 \begin{Bmatrix} 1/\sqrt{Y_j^{\text{TE}}} \\ \sqrt{Y_j^{\text{TM}}} \end{Bmatrix} u_j(z) \exp[-i(\omega t - \beta y)], \quad (\text{B.1})$$

where

$$u_j(z) = a_j \exp(ik_{zj}z) + b_j \exp(-ik_{zj}z), \quad (\text{B.2})$$

and  $a_j$  and  $b_j$  are the field amplitudes,  $Y_j^{\text{TE}} = k_{zj}/k_0\mu_j$  and  $Y_j^{\text{TM}} = k_0\varepsilon_j/k_{zj}$  are the wave admittances,  $k_0 = \omega/c$  is the wavenumber in free space, and  $k_{zj}$  is the transverse wavenumber which takes on discrete values in each slab and can be written as

$$k_{zj} = (k_0^2 n_j^2 - \beta^2)^{1/2} = k_0 (n_j^2 - n_{eff}^2)^{1/2}. \quad (\text{B.3})$$

Here  $n_j$  takes on values  $n_g$  for the core layer, and  $n_\Psi$  and  $n_\Upsilon$  for the  $\Psi$  and  $\Upsilon$  cladding layers, respectively.

The field amplitudes for the structure input and output are evaluated as [18, 19, 20]

$$\begin{bmatrix} a_0 \\ b_0 \end{bmatrix} = \mathbf{T}_\Sigma \begin{bmatrix} a_N \\ b_N \end{bmatrix} = \left( \underbrace{\mathbf{T}_\Psi \mathbf{T}_\Upsilon \mathbf{T}_\Upsilon \mathbf{T}_\Psi \mathbf{T}_\Psi \mathbf{T}_\Upsilon \dots}_{N} \right) \begin{bmatrix} a_N \\ b_N \end{bmatrix}, \quad (\text{B.4})$$

where the total transfer matrix  $\mathbf{T}_\Sigma$  is obtained by multiplying in the appropriate order the matrices corresponding to each layer in the structure.

The matrices  $\mathbf{T}_\Psi$  and  $\mathbf{T}_\Upsilon$  are the particular transfer matrices of rank 2 of the  $\Psi$  and  $\Upsilon$  layers in cladding with their corresponding thicknesses  $d_\Psi$  and  $d_\Upsilon$ . They are

$$\mathbf{T}_\Psi = \mathbf{T}_{01} \mathbf{P}_1(d_\Psi) \mathbf{T}_{10}, \quad \mathbf{T}_\Upsilon = \mathbf{T}_{02} \mathbf{P}_2(d_\Upsilon) \mathbf{T}_{20}, \quad (\text{B.5})$$

where  $\mathbf{T}_{0j}$  and  $\mathbf{T}_{j0}$  ( $j = 1, 2$ ) are the transfer matrices of the layer interfaces with outer half-spaces, and  $\mathbf{P}_j(d)$  are the propagation matrices through the corresponding layer. The elements of the matrices  $\mathbf{T}_{0j}$  and  $\mathbf{T}_{j0}$  are determined by solving the boundary-value problem related to the field components (B.1):

$$\mathbf{T}_{pv} = \frac{1}{2\sqrt{Y_p Y_v}} \begin{bmatrix} Y_p + Y_v & \pm(Y_p - Y_v) \\ \pm(Y_p - Y_v) & Y_p + Y_v \end{bmatrix}, \quad (\text{B.6})$$

$$\mathbf{P}_j(d) = \begin{bmatrix} \exp(-ik_{zj}d) & 0 \\ 0 & \exp(ik_{zj}d) \end{bmatrix}, \quad (\text{B.7})$$

where the upper sign ‘+’ relates to the TE wave, while the lower sign ‘−’ relates to the TM wave.

Finally, the reflection coefficient of the layer stack is determined by the expression

$$R = |R| \exp(i\phi) = (b_0/a_0)|_{b_N=0} = -t_{21}/t_{22}, \quad (\text{B.8})$$

where  $t_{mn}$  are the elements of the transfer matrix  $\mathbf{T}_\Sigma$ , and  $\phi$  is the phase of the reflected light.

## References

- [1] A. Snyder, J. Love, Optical Waveguide Theory, Science paperbacks, Springer, 1983.  
URL [https://books.google.com.ua/books?id=gIQB\\_hzB0SMC](https://books.google.com.ua/books?id=gIQB_hzB0SMC)

- [2] P. Yeh, A. Yariv, Bragg reflection waveguides, *Optics Communications* 19 (3) (1976) 427–430.  
doi:[http://dx.doi.org/10.1016/0030-4018\(76\)90115-2](http://dx.doi.org/10.1016/0030-4018(76)90115-2).  
URL <http://www.sciencedirect.com/science/article/pii/0030401876901152>
- [3] S. Johnson, M. Ibanescu, M. Skorobogatiy, O. Weisberg, T. Enghes, M. Soljacic, S. Jacobs, J. Joannopoulos, Y. Fink, Low-loss asymptotically single-mode propagation in large-core omniguided fibers, *Opt. Express* 9 (13) (2001) 748–779. doi:10.1364/OE.9.000748.  
URL <http://www.opticsexpress.org/abstract.cfm?URI=oe-9-13-748>
- [4] P. Russell, Photonic crystal fibers, *Science* 299 (5605) (2003) 358–362.  
arXiv:<http://www.sciencemag.org/content/299/5605/358.full.pdf>,  
doi:10.1126/science.1079280.  
URL <http://www.sciencemag.org/content/299/5605/358.abstract>
- [5] B. R. West, A. S. Helmy, Properties of the quarter-wave Bragg reflection waveguide: Theory, *J. Opt. Soc. Am. B* 23 (6) (2006) 1207–1220.  
doi:10.1364/JOSAB.23.001207.  
URL <http://josab.osa.org/abstract.cfm?URI=josab-23-6-1207>
- [6] J. Li, K. S. Chiang, Guided modes of one-dimensional photonic bandgap waveguides, *J. Opt. Soc. Am. B* 24 (8) (2007) 1942–1950.  
doi:10.1364/JOSAB.24.001942.  
URL <http://josab.osa.org/abstract.cfm?URI=josab-24-8-1942>
- [7] J. Li, K. S. Chiang, Light guidance in a photonic bandgap slab waveguide consisting of two dielectric layers, *Optics Communications* 281 (23) (2008) 5797–5803.  
doi:<http://dx.doi.org/10.1016/j.optcom.2008.08.040>.  
URL <http://www.sciencedirect.com/science/article/pii/S0030401808008432>
- [8] Y. Li, Y. Xi, X. Li, W.-P. Huang, A single-mode laser based on asymmetric Bragg reflection waveguides, *Opt. Express* 17 (13) (2009) 11179–11186. doi:10.1364/OE.17.011179.  
URL <http://www.opticsexpress.org/abstract.cfm?URI=oe-17-13-11179>
- [9] B. Nistad, M. W. Haakestad, J. Skaar, Dispersion properties of planar Bragg waveguides, *Optics Communications* 265 (1) (2006) 153–160.

doi:<http://dx.doi.org/10.1016/j.optcom.2006.03.014>.

URL <http://www.sciencedirect.com/science/article/pii/S0030401806002252>

- [10] B. Pal, S. Ghosh, R. Varshney, S. Dasgupta, A. Ghatak, Loss and dispersion tailoring in 1D photonics band gap Bragg reflection waveguides: Finite c Optical and Quantum Electronics 39 (12–13) (2007) 983–993. doi:10.1007/s11082-007-9160-y. URL <http://dx.doi.org/10.1007/s11082-007-9160-y>
- [11] P. Abolghasem, A. S. Helmy, Matching layers in Bragg reflection waveguides for enhanced nonlinear interaction, Quantum Electronics, IEEE Journal of 45 (6) (2009) 646–653. doi:10.1109/JQE.2009.2013118.
- [12] J.-S. I, Y. Park, H. Jeon, Optimal design for one-dimensional photonic crystal waveguide, J. Lightwave Technol. 22 (2) (2004) 509. URL <http://jlt.osa.org/abstract.cfm?URI=jlt-22-2-509>
- [13] E. Maciá, The role of aperiodic order in science and technology, Reports on Progress in Physics 69 (2) (2006) 397. URL <http://stacks.iop.org/0034-4885/69/i=2/a=R03>
- [14] O. Shramkova, Y. Olkhovskiy, Electromagnetic wave transmission and reflection by a quasi-periodic structure, Physica B: Condensed Matter 406 (8) (2011) 1415 – 1419. doi:<http://dx.doi.org/10.1016/j.physb.2011.01.041>. URL <http://www.sciencedirect.com/science/article/pii/S0921452611000780>
- [15] V. I. Fesenko, V. R. Tuz, P. P. Rocha Garcia, I. A. Sukhoivanov, Dispersion properties of a one-dimensional aperiodic OmniGuide structure, Proc. SPIE 9200 (2014) 920017–920017–7. doi:10.1117/12.2060525. URL <http://dx.doi.org/10.1117/12.2060525>
- [16] V. I. Fesenko, V. R. Tuz, I. A. Sukhoivanov, Terahertz aperiodic multilayered structure arranged according to the Kolakoski sequence, in: M. F. Pereira, O. Shulika (Eds.), Terahertz and Mid Infrared Radiation: Detection of Explosives and CBRN (Using Terahertz), NATO Science for Peace and Security Series B: Physics and Biophysics, 2014.
- [17] V. I. Fesenko, Omnidirectional reflection from generalized Kolakoski multilayers, Progress In Electromagnetics Research M 41 (2015) 33–41. doi:10.2528/PIERM14121103.

- [18] V. R. Tuz, Optical properties of a quasi-periodic generalized Fibonacci structure of chiral and J. Opt. Soc. Am. B 26 (4) (2009) 627–632.  
doi:10.1364/JOSAB.26.000627.  
URL <http://josab.osa.org/abstract.cfm?URI=josab-26-4-627>
- [19] V. Tuz, V. Kazanskiy, Electromagnetic scattering by a quasiperiodic generalized multilayer F Waves in Random and Complex Media 19 (3) (2009) 501–508.  
doi:10.1080/17455030902780445.  
URL <http://www.tandfonline.com/doi/abs/10.1080/17455030902780445>
- [20] V. R. Tuz, O. D. Batrakov, Localization and polarization transformation of waves by a symme Journal of Modern Optics 57 (21) (2010) 2114–2122.  
doi:10.1080/09500340.2010.522261.  
URL <http://dx.doi.org/10.1080/09500340.2010.522261>
- [21] V. I. Fesenko, Aperiodic birefringent photonic structures based on Ko-lakoski sequence, Waves in Random and Complex Media 24 (2) (2014) 174–190. doi:10.1080/17455030.2014.890764.
- [22] M. Kohmoto, B. Sutherland, K. Iguchi, Localization of optics: Quasiperiodic media, Phys. Rev. Lett. 58 (1987) 2436–2438. doi:10.1103/PhysRevLett.58.2436.  
URL <http://link.aps.org/doi/10.1103/PhysRevLett.58.2436>
- [23] N.-h. Liu, Propagation of light waves in Thue-Morse dielectric multilayers, Phys. Rev. B 55 (1997) 3543–3547. doi:10.1103/PhysRevB.55.3543.  
URL <http://link.aps.org/doi/10.1103/PhysRevB.55.3543>
- [24] B. Sing, Kolakoski sequences - an example of aperiodic order, Journal of Non-Crystalline Solids 334 (2004) 100–104.  
doi:<http://dx.doi.org/10.1016/j.jnoncrysol.2003.11.021>.  
URL <http://www.sciencedirect.com/science/article/pii/S0022309303008524>
- [25] V. I. Fesenko, V. R. Tuz, O. V. Shulika, I. A. Sukhoivanov, Dispersion properties of a nanophotonic Bragg waveguide with finite aperiodic cladding, ArXiv e-prints arXiv:1510.03470.  
URL <http://adsabs.harvard.edu/abs/2015arXiv151003470F>
- [26] S. Adachi, GaAs, AlAs, and  $\text{Al}_x\text{Ga}_{1-x}\text{As}$ : Material parameters for use in research and device Journal of Applied Physics 58 (3) (1985) R1–R29.



doi:<http://dx.doi.org/10.1063/1.336070>.

URL <http://scitation.aip.org/content/aip/journal/jap/58/3/10.1063/1.336070>

- [27] A. Argyros, Guided modes and loss in Bragg fibres, *Opt. Express* 10 (24) (2002) 1411–1417. doi:[10.1364/OE.10.001411](https://doi.org/10.1364/OE.10.001411).  
URL <http://www.opticsexpress.org/abstract.cfm?URI=oe-10-24-1411>
- [28] M. Özer, A. Čenys, Y. Polatoglu, G. Hacibekiroglu, E. Akat, A. Valaristos, A. Anagnostopoulos, Bifurcations of Fibonacci generating functions, *Chaos, Solitons & Fractals* 33 (4) (2007) 1240–1247.  
doi:<http://dx.doi.org/10.1016/j.chaos.2006.01.095>.  
URL <http://www.sciencedirect.com/science/article/pii/S0960077906001457>
- [29] L. Moretti, I. Rea, L. De Stefano, I. Rendina, Periodic versus aperiodic: Enhancing the sensitivity of porous silicon based optical sensors, *Applied Physics Letters* 90 (19) (2007) 191112.  
doi:<http://dx.doi.org/10.1063/1.2737391>.  
URL <http://scitation.aip.org/content/aip/journal/apl/90/19/10.1063/1.2737391>